Am J Transl Res 2023;15(7):4573-4586
www.ajtr.org /ISSN:1943-8141/AJTR0150346

Original Article

A novel large animal model of posttraumatic osteoarthritis induced by inflammation with mechanical stability

Changqi Sun[1*], Kenny Chang[1*], Braden C Fleming[1], Brett D Owens[1], Jillian E Beveridge[2], Andrew Gage[1], Rachel C Talley-Bruns[1], Scott McAllister[1], Meggin Q Costa[1], Megan P Pinette[1], Madalyn Hague[1], Janine Molino[1], Ying Xiao[1], Shaolei Lu[1], Lei Wei[1]

[1]Department of Orthopaedics, Warren Alpert Medical School of Brown University/Rhode Island Hospital, Providence, RI, USA; [2]Cleveland Clinic Biomedical Engineering Department, Cleveland, OH, USA. [*]Equal contributors.

Received March 24, 2023; Accepted June 7, 2023; Epub July 15, 2023; Published July 30, 2023

Abstract: Objectives: Animal models are needed to reliably separate the effects of mechanical joint instability and inflammation on posttraumatic osteoarthritis (PTOA) pathogenesis. We hypothesized that our modified intra-articular drilling (mIAD) procedure induces cartilage damage and synovial changes through increased inflammation without causing changes in gait. Methods: Twenty-four Yucatan minipigs were randomized into the mIAD (n=12) or sham control group (n=12). mIAD animals had two osseous tunnels drilled into each of the tibia and femur adjacent to the anterior cruciate ligament (ACL) attachment sites on the left hind knee. Surgical and contralateral limbs were harvested 15 weeks post-surgery. Cartilage degeneration was evaluated macroscopically and histologically. Synovial changes were evaluated histologically. Interleukin-1 beta (IL-1β), nuclear factor kappa B (NF-κB), and tumor necrosis factor alpha (TNF-α) mRNA expression levels in the synovial membrane were measured using quantitative real-time polymerase chain reaction. IL-1β and NF-κB levels in chondrocytes were assessed using immunohistochemistry. Load asymmetry during gait was recorded by a pressure-sensing walkway system before and after surgery. Results: The mIAD surgical knees demonstrated greater gross and histological cartilage damage than contralateral (P<.01) and sham knees (P<.05). Synovitis was present only in the mIAD surgical knee. Synovial inflammatory marker (IL-1β, NF-κB, and TNF-α) expression was three times higher in the mIAD surgical knee than the contralateral (P<.05). Chondrocyte IL-1β and NF-κB levels were highest in the mIAD surgical knee. In general, there were no significant changes in gait. Conclusions: The mIAD model induced PTOA through inflammation without affecting gait mechanics. This large animal model has significant applications for evaluating the role of inflammation in PTOA and for developing therapies aimed at reducing inflammation following joint injury.

Keywords: Posttraumatic osteoarthritis, inflammation, gait, synovium, minipig

Introduction

Posttraumatic osteoarthritis (PTOA) refers to cartilage degeneration caused by some form of joint trauma such as injury or surgery [1, 2]. PTOA comprises 12% of the overall prevalence of osteoarthritis cases and disproportionately affects the youth population because they sustain more recreation-related injuries [1, 2]. A range of injuries, such as intra-articular fractures, dislocations, and ligamentous disruptions, are linked to the development of PTOA [3-6]. Unfortunately, surgical treatment that attempts to restore joint mechanics does not fully reduce the risk of PTOA [5, 7-9]. The pathogenesis of PTOA following surgical repair is hypothesized to be caused by (1) residual changes in joint loading leading to mechanical cartilage damage and (2) inflammatory mediators, such as interleukin-1 beta (IL-1β), nuclear factor kappa B (NF-κB), and tumor necrosis factor alpha (TNF-α), that initiate and maintain biological cartilage degradation through a catabolic cascade [10-14]. It remains unknown which factor is dominant.

Large animals such as the Yucatan minipig have been used to study PTOA because of their

sufficient joint tissue for molecular analysis, similar joint biomechanics compared to humans, and ease of surgery [15-20]. In addition, the minipig model exhibits features of osteoarthritis common to those seen in humans [16, 21, 22]. However, large animal models, such as anterior cruciate ligament (ACL) transection or medial meniscus destabilization (DMM), cannot be used to reliably distinguish the role of inflammation because of the interaction between mechanical and biological changes that lead to cartilage damage [10, 11]. Due to the potentially modifiable nature of early-stage inflammation, there is an impetus to develop pre-clinical large animal models that can reliably isolate the role of inflammation on PTOA development and allow for the specific study of anti-inflammatory therapies. As a result, Heard et al. developed an "idealized" ACL reconstruction (IACLR) model to study the PTOA-initiating effects of inflammatory mediators while controlling for mechanical changes in sheep [23]. In the model, the femoral attachment of the native ACL was cored out and immediately reattached as an ideal graft to restore normal biomechanics [23]. However, while attempting to replicate the procedure on minipigs, we found that the coring procedure induced additional damage to the joint, including major trauma to the lateral extra-articular structures and cutting some of the fibers of the normal ACL.

In this study, we developed a modified intra-articular drilling model (mIAD) in the minipig to isolate and study the effects of inflammation in PTOA [14]. We drilled two osseous tunnels through both the tibia and femur adjacent to the intra-articular tibial and femoral ACL insertions on non-articulating surfaces, thus avoiding the risk of mechanically damaging the intra-articular ligaments, the lateral extra-articular structures, or articular cartilage. We hypothesize that the mIAD procedure would induce cartilage damage in the surgical knee through inflammatory factors but would not cause mechanical changes during gait.

Materials and methods

Study design

The study was approved by the Institutional Animal Care and Use Committee of our institution and the Animal Care and Use Review Office from the Department of Defense (Protocol number: 19-04-0001). The study was designed to meet the ARRIVE guidelines [24]. Twenty-four Yucatan minipigs (age 15-16 months old, 12 castrated males, 12 females, weight 54±6.5 kg) were randomly allocated to an mIAD surgical (n=12) and sham control group (n=12) with each group counterbalanced by sex. All animals were housed individually in adjacent pens (minimum pen size of 2.1 m^2) for 15 weeks.

Surgical technique

The animals were anesthetized, and a medial arthrotomy was performed on the left hind knee to access the ACL. A commercial drill system (Cordless Driver 4; Stryker, Kalamazoo, MI, USA) was used to perform the drilling procedure with Kirschner wires. Two osseous tunnels 2 mm in diameter and 15 mm deep were drilled into the tibial bone adjacent to the anterior and posterior edges of the tibial ACL insertion. The drilling procedure was repeated at the anterior medial and posterior lateral edges of the femoral ACL insertion similarly to the procedure previously described by Huebner *et al.* in rabbits [14]. The wound was then irrigated with sterile saline. The knee was closed in layers with buried absorbable sutures (Vicryl, Ethicon, Raritan, NJ, USA): Arthrotomy: 0, interrupted; Bursa: 2-0, running; Subcutaneous tissue: 2-0, interrupted; and Subcuticular layer: 3-0 interrupted. Post-operative pain was managed using a fentanyl patch placed on the dorsum of the pig for 3 days. Animals were treated with ondansetron, an anti-vomiting agent, immediately post-operation. Animals were kept in pens for the duration of the study. They were not forced to exercise, though they appeared active when checked daily. The sham control group underwent the same arthrotomy procedure but without the intra-articular drilling. The animals were euthanized with a euthanasia solution (Beuthanasia-D Special, Merck, Madison, WI, USA) at 15 weeks, and both hind knees were harvested. The contralateral knee was used as an internal control.

Macroscopic cartilage assessment

The medial and lateral articulating surfaces of the tibial plateau and femoral condyle of both surgical and contralateral mIAD hind limbs and the surgical left limbs of the sham animals were

stained with India ink and photographed. The length and width of India Ink-stained lesions were measured using calipers. The lesion area was approximated as an ellipse [25].

Histological preparation

Osteochondral slabs from the central medial and lateral compartments of the tibial plateau and femoral condyles were dissected from the knee. Each slab covered the entire width of the tibial plateau and femoral condyles (medial and lateral separate). They were fixed in 10% formalin for 48 hours and stored in 70% ethanol. The tissue was rinsed in running tap water for 30 minutes, placed in cassettes, and transferred to buffered formic acid decalcification solution at room temperature (20% formic acid, 10% sodium citrate in dH_2O). Bone outside the region of interest was scored with a razor blade to improve reagent penetration as needed. Bones were bifurcated along the long axis on day 3. The solution was changed every 3-4 days, and the decalcification progress was monitored by X-ray. The endpoint was reached at 7-10 days, depending on tissue size. Decalcified tissue was rinsed in running tap water for 30 minutes and then transferred to 70% ethanol at room temperature. The tissue was loaded onto an automated tissue processor for dehydration and paraffin infiltration under pressure/vacuum. After infiltration, the tissue was trimmed to fit into embedding molds and oriented so that the two halves were embedded bifurcation-side down in the embedding mold. Embedded blocks were stored in a block filing box protected from light at room temperature. Embedded samples were sectioned with a rotary microtome at 6 μm onto positively charged slides. Slides were stained with Safranin O-fast green.

Microscopic cartilage assessment

Slides stained with Safranin O-fast green were scored according to a modified Osteoarthritis Research Society International (OARSI) grading system that characterized the severity of cartilage damage in large animals [15]. Four items, structure (0-10), chondrocyte density (0-4), cell cloning (0-4), and interterritorial Safranin O-fast green (0-4), were evaluated by 6 blinded evaluators [15]. The extent of surface area affected by structural damage was assessed according to the OARSI grading system [15].

Synovial tissue preparation

We sampled synovial tissue from the suprapatellar fold so that the sub-intimal fibrosis could be scored. Frozen synovium sections (10 μm) were prepared for hematoxylin & eosin staining. Synovium features were evaluated using a modified OARSI grading system [15]. Three items, intimal hyperplasia (0-3), inflammatory cell infiltration (0-3), and vascularity (0-3), were evaluated by three blinded evaluators [15]. At least three randomly selected areas of the synovium were scored per section for each observation.

Real-time quantitative reverse transcription PCR for inflammatory mediators

Gene expression levels of IL-1β, NF-κB, and TNF-α from synovial membranes were analyzed using real-time quantitative reverse transcriptase-polymerase chain reaction (qRT-PCR) according to published protocols (iQ SYBR Green Supermix, Bio-Rad, Hercules, CA, USA). After synovial membrane tissues were homogenized in TRIzol reagent (cat# 15596026, Invitrogen, Waltham, MA, USA) using a homogenizer, total RNA was extracted with the TRIzol reagent and purified further using the RNeasy Mini Kit (cat# 74004, Qiagen, Hilden, Germany). Gene expression was measured through two methods: first-strand cDNA synthesis using a reverse transcription kit (cat# 1708890, Bio-Rad, Hercules, CA, USA) and qRT-PCR using the iQ™ SYBR Green Supermix kit (cat# 170-8887, Bio-Rad, Hercules, CA, USA) in a real-time PCR system (CFX Connect, Bio-Rad, Hercules, CA, USA). A total of 1 μg of RNA was used for cDNA synthesis.

Priming was conducted at 25°C for five minutes. Reverse transcription was conducted at 40°C for 20 minutes. Reverse transcriptase inactivation was done at 95°C for one minute. For qRT-PCR testing, 18S ribosomal RNA, a well-known reference gene, was used as an internal control. Swine-specific primers were designed and synthesized by Integrated DNA Technologies (IDT, Coralville, IA, USA) as specified in **Table 1**. PCR was performed for 40 cycles after an initial denaturation step at 95°C for 3 minutes. Each cycle involved an additional denaturation step for 15 seconds at 95°C, annealing for 60 seconds at 55°C or 58°C, and extension for 40 seconds at 72°C. The reaction

Table 1. Primers used for real-time quantitative reverse transcription polymerase chain reaction evaluation of inflammatory mediators in the synovial membrane

Target gene	Primer Sequences	
IL-1β	Forward	5'-CTG CAA ACT CCA GGA CAA AGA-3'
	Reverse	5'-GGG TGG CAT CAC AGA AAA-3'
TNF-α	Forward	5'-CCT ACT GCA CTT CGA GGT TATC-3'
	Reverse	5'-ACG GGC TTA TCT GAG GTT TG-3'
NF-κB	Forward	5'-ACT TGC CAG ACA CAG ATG AC-3'
	Reverse	5'-GTC GGT GGG TCC ATT GAA A-3'
18S	Forward	5'-GTA ACC CGT TGA ACC CCA TT-3'
	Reverse	5'-CCA TCC AAT CGG TAG TAG CG-3'

was terminated at 70°C after a 10-minute extension. Three independent PCR experiments were performed to obtain the relative level of expression for each gene.

Immunohistochemistry

Cartilage specimens were analyzed using the Immunohistochemistry Detection System (TL-015-HD, Epredia, Kalamazoo, MI, USA) to assess IL-1β and NF-κB levels. Staining was done according to the manufacturer's instructions. The sections were digested with 5 mg/mL of hyaluronidase in phosphate-buffer saline. The sections were then incubated with 20.8 μg/mL of antibody against rabbit NF-κB (cat# 10745-1-AP Proteintech Group, Rosemont, IL, USA) and 40 μg/mL of antibody against rabbit IL-1β (cat# 420B, Invitrogen, Waltham, MA, USA) at 4°C overnight. The immunohistochemistry kit utilizes a universal secondary antibody formulation conjugated to an enzyme-labeled polymer that recognizes rabbit antibodies. Coverslips were then mounted for visualization under the microscope.

Gait assessment

Gait mechanics indicators were used as a proxy measure of joint instability. Load asymmetry during gait was recorded by a pressure sensing walkway system (23" × 130") (Tekscan, Boston, MA, USA) before (week 0) and four times after surgery (weeks 4, 8, 12, and 15). Before gait testing, the walkway system was calibrated following the manufacturer's instructions [26]. During gait testing, the loading curves were checked to ensure the system was operating properly. Five successful walkway trials were performed and recorded at each time point for each animal. The differential hind limb loading between the left (surgical) and right hind limb was calculated across gait cycles and expressed as a ratio for six gait parameters: maximum force, contact area, peak pressure, impulse, stance time, and swing time [26].

Statistical methods

Data were imported into statistical software (SAS version 9.4; SAS Institute Inc., Cary, NC) for hypothesis testing. Generalized estimating equations (GEE) were used to compare macroscopic damage, microscopic damage, synovial membrane changes, qRT-PCR levels, and gait ratios across experimental conditions. GEEs were chosen as the analytic method because they allow appropriate handling of data structures associated with repeated and/or clustered measurements and maximize the information from subjects with missing observations. The Gaussian distribution with an identity link was used for the macroscopic cartilage damage, synovial qRT-PCR, and gait measures while a binomial distribution with a logit link was used for the microscopic cartilage damage and microscopic synovial membrane measures. These distributions and link functions were determined by examining the distribution of the dependent variables and the model residuals. Synovial qRT-PCR data was analyzed as cycles to threshold and then transposed into fold-changes for interpretation. Classical sandwich estimators were used to protect against possible model misspecification. Pairwise comparisons between experimental conditions were conducted within the models via orthogonal contrasts. The Holm test was used for multiple comparisons to maintain a two-tailed family-wise alpha of 0.05 across the comparisons tested. An adjusted *P*-value <0.05 was used to determine statistical significance. Power for the microscopic OARSI damage scores was estimated to be 80% for detecting a 6-point difference using a one-tailed pairwise comparison. A sample size of 12 minipigs per group allowed us to maintain at least 80% power for all hypothesis tests.

Results

Macroscopic cartilage assessment

All animals in the mIAD group showed macroscopic cartilage degeneration in the surgical

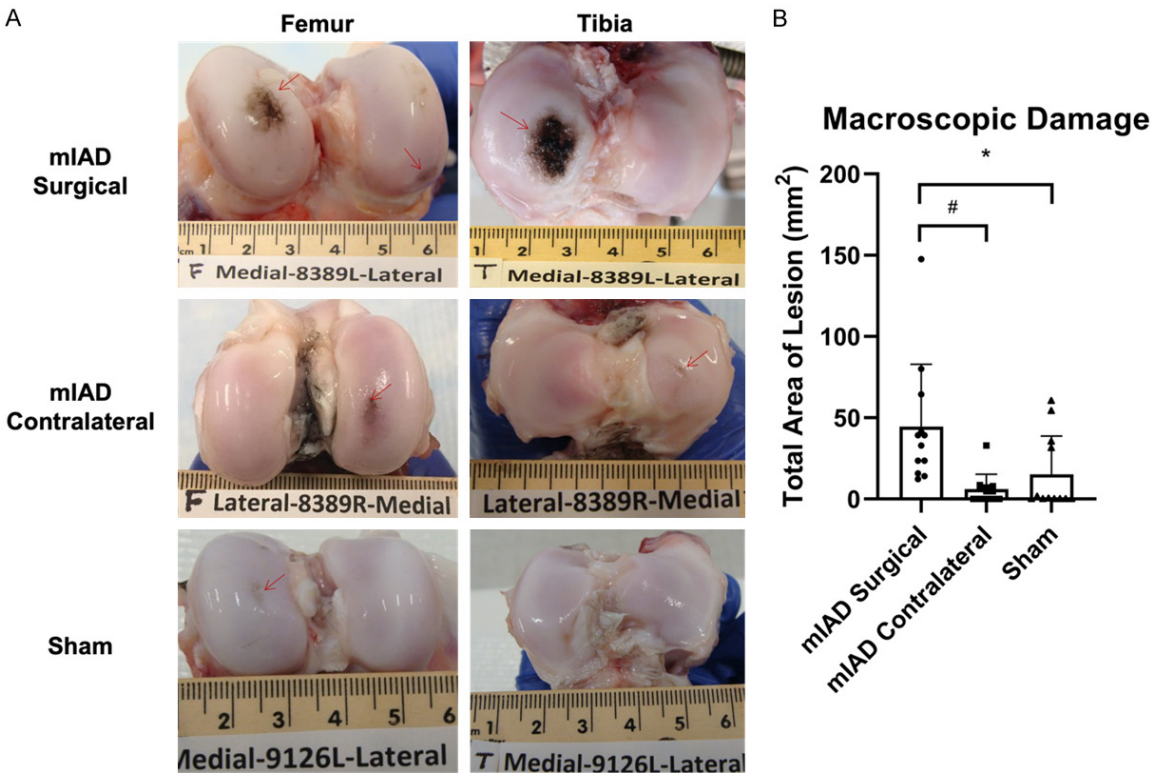

Figure 1. Macroscopic cartilage damage. A. Images of median lesion areas stained with India Ink for each group: modified intra-articular drilling (mIAD) surgical, mIAD contralateral, and sham. B. Total lesion area for each group: mIAD surgical, mIAD contralateral, and sham. Error bars represent the standard deviation. * indicates significant differences between mIAD surgical and sham. # indicates significant differences between mIAD surgical and contralateral.

knee (**Figure 1A**). Seven of the twelve animals showed minor degeneration in the mIAD contralateral knee (**Figure 1A**). In the sham group, six of the twelve animals showed moderate degeneration in the surgical knee (**Figure 1A**). Mean lesion area was greater in the mIAD surgical knee compared with the mIAD contralateral (P=.004) and sham surgical knees (P=.049) (**Figure 1B**). There were no significant differences in total lesion area between the mIAD contralateral and sham surgical knees (P=.192) (**Figure 1B**). In the mIAD surgical knee, lesions were predominantly located in the medial femoral condyle (MFC) (17.4±13.5 mm^2) and medial tibial plateau (MTP) (19.7±16.9 mm^2), with some present in the lateral femoral condyle (LFC) (4.5±7.0 mm^2) and lateral tibial plateau (LTP) (2.9±6.9 mm^2). In both the mIAD contralateral and sham surgical knees, there were occasional slight lesions in the MFC (mIAD contralateral: 5.3±7.8 mm^2; sham: 8.2±15.0 mm^2) and MTP (mIAD contralateral: 0.7±1.5 mm^2; sham: 4.2±8.1 mm^2).

Microscopic cartilage assessment

The total severity of cartilage damage score (MFC, MTP, LFC, and LTP) was significantly higher in the mIAD surgical knee compared with the mIAD contralateral (P<.001) and sham surgical knees (P=.010) (**Figure 2A-D**). There was no significant difference in the severity of microscopic damage between the mIAD contralateral and sham surgical knees (P=.431) (**Figure 2D**). The total extent of surface area damaged score was significantly higher in the mIAD surgical knee compared with the mIAD contralateral (P<.001) and sham surgical knees (P=.013) (**Figure 2E**). There was no significant difference in the extent of surface area damaged between the mIAD contralateral and sham surgical knees (P=.664) (**Figure 2E**). Furthermore, in the mIAD surgical knee, the severity of microscopic damage score was higher in the medial compartment (MFC: 9.3±7.4; MTP: 8.0±4.6) than the lateral compartment (LFC: 3.7±5.9; LTP: 2.6±2.4). The extent of surface area damaged

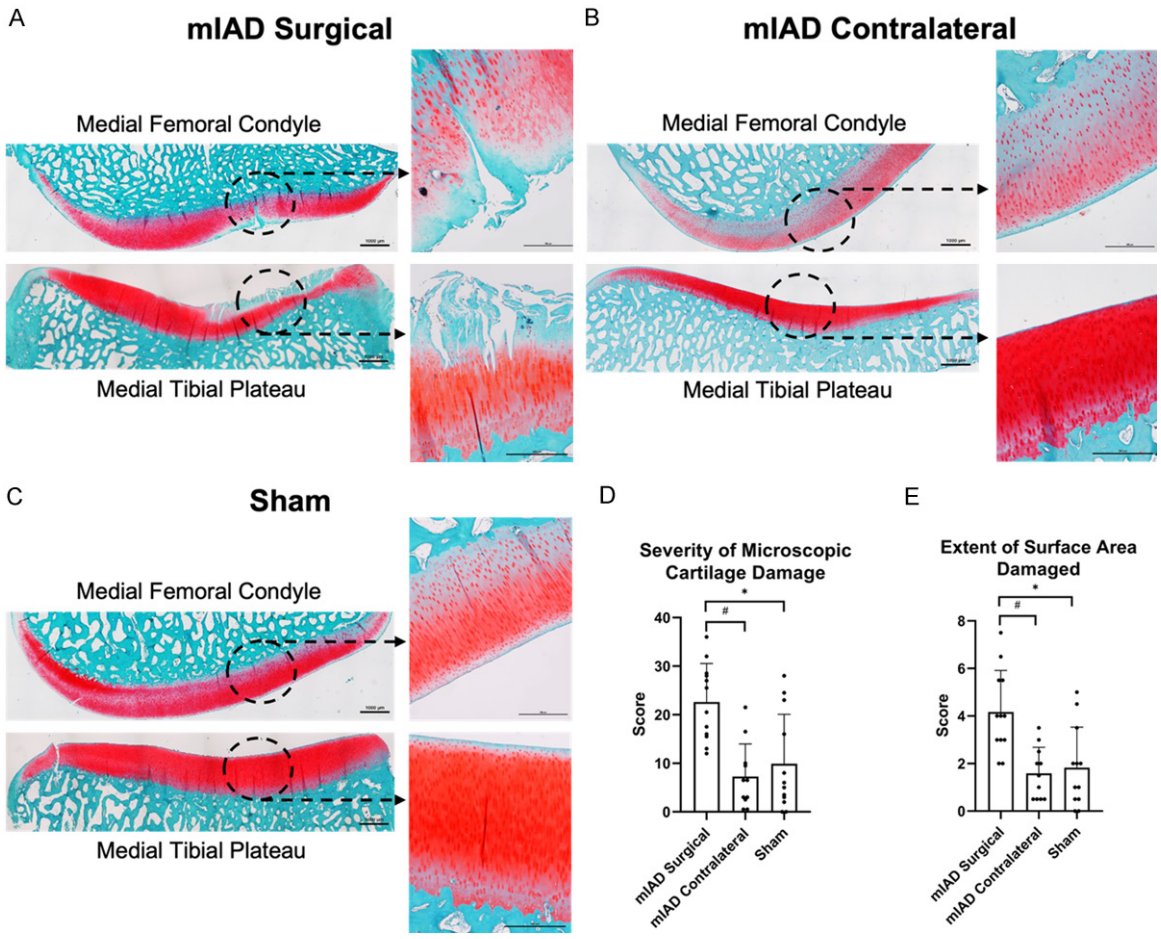

Figure 2. Microscopic cartilage damage. Histological images of the median medial femoral condyle and medial tibial plateau stained with Safranin O-fast green for (A) modified intra-articular drilling (mIAD) surgical, (B) mIAD contralateral, and (C) sham. (D) Summed modified Osteoarthritis Research Society International (OARSI) scores from all compartments of the joint measuring structure, chondrocyte density, cell cloning, and interterritorial staining. (E) Summed scores for the extent of surface area damaged. Error bars represent the standard deviation. * indicates significant differences between mIAD surgical and sham. # indicates significant differences between mIAD surgical and contralateral.

score followed a similar pattern (MFC: 1.2±1.2; MTP: 1.9±1.3; LFC: 0.67±0.9; 0.6±0.6). This was similarly observed for the mIAD contralateral and sham surgical knees.

In the medial compartment of the mIAD surgical knee, we observed degeneration affecting 10-25% of the cartilage surface area, severe surface irregularities, decrease in chondrocyte density, formation of chondrocyte clusters, decreased interterritorial Safranin-O staining to the mid zone, and occasional erosions to the deep zone (**Figure 2A**). In the mIAD contralateral (**Figure 2B**) and sham surgical knees (**Figure 2C**), we observed degeneration affecting less than 10% of the cartilage surface area, slight to moderate surface irregularities, minimal changes in chondrocyte density, minimal chondrocyte cell cloning, and no changes in interterritorial Safranin-O staining.

Changes in the synovial membrane

We observed moderate diffuse hyperplasia, diffuse inflammatory cell infiltration, and the presence of vascular elements in the mIAD surgical knees (**Figure 3A**). On the other hand, we observed minimal changes in hyperplasia, inflammatory cell infiltration, and vascularity in the mIAD contralateral knees (**Figure 3B**) and sham surgical knees (**Figure 3C**). The synovial membrane scores of the mIAD surgical knees

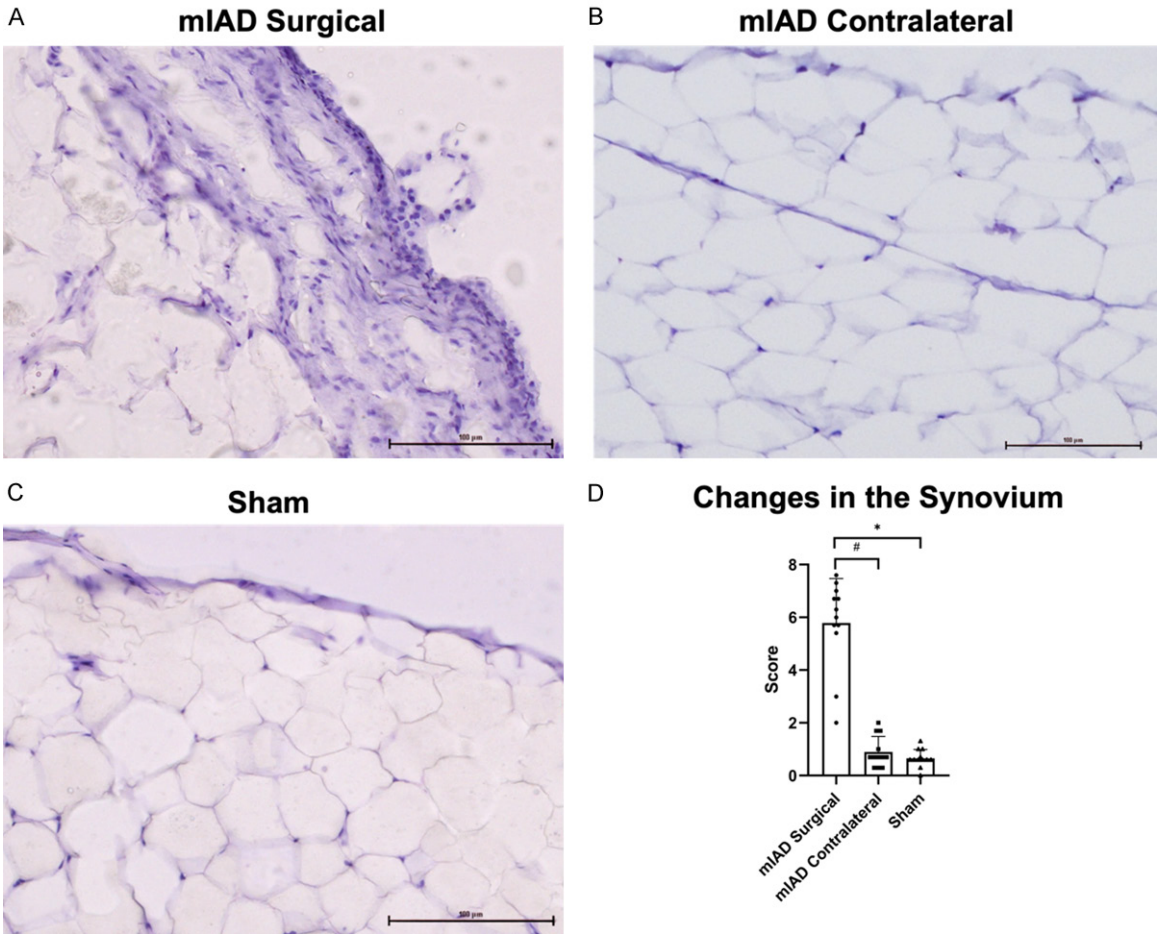

Figure 3. Synovitis from modified intra-articular drilling (mIAD) surgery. (A) Histological images of the median synovial membrane from the suprapatellar fold for mIAD surgical, (B) mIAD contralateral, and (C) sham. (D) Microscopic synovial membrane scores. Error bars represent the standard deviation. * indicates significant differences between mIAD surgical and sham. # indicates significant differences between mIAD surgical and contralateral.

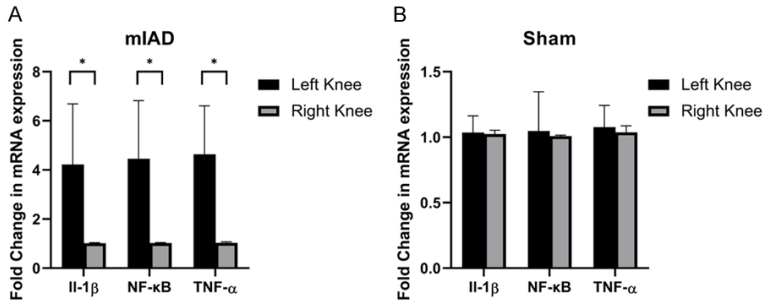

Figure 4. Differential mRNA expression of inflammatory mediators in the synovial membrane of the modified intra-articular drilling (mIAD) and sham groups. A. Fold change of interleukin-1 beta (IL-1β), nuclear factor kappa B (NF-κB), and tumor necrosis factor alpha (TNF-α) mRNA in the mIAD group. B. Fold change of IL-1β, NF-κB, and TNF-α mRNA in the sham group. (Black = left knee, grey = right knee). Error bars represent the standard deviation. * indicates significant differences.

were significantly higher than the mIAD contralateral (P<.001) and sham surgical knees (P<.001), while the synovial membrane scores of the contralateral knees were not significantly different from the sham surgical knee (P=.180) (**Figure 3D**).

The contralateral knees of each animal were used as internal controls to assess the changes in IL-1β, NF-κB, and TNF-α mRNA expression levels in the synovial membranes within individual animals. Expression of IL-1β, NF-κB, and TNF-α mRNA in the synovial membrane of mIAD surgical knee was, on average, three times the level in the mIAD contralateral knee (IL-1β: P=.031; TNF-α: P=.002; NF-κB:

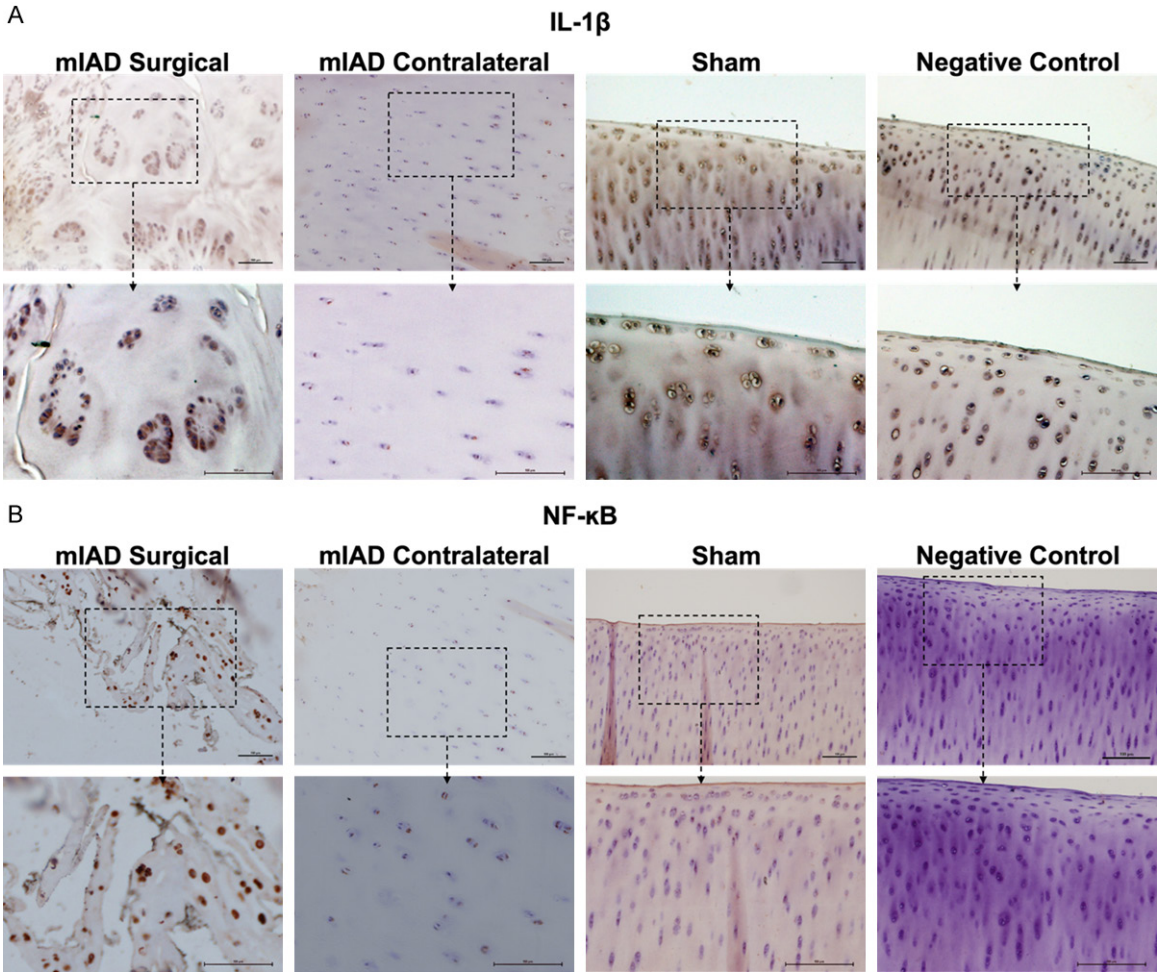

Figure 5. Interleukin-1 beta (IL-1β) and nuclear factor kappa B (NF-κB) in chondrocytes of the medial femoral condyle. A. Representative IL-1β immunohistochemistry staining for modified intra-articular drilling (mIAD) surgical, mIAD contralateral, sham, and negative control. B. Representative NF-κB immunohistochemistry staining.

P=.020) (**Figure 4A**). No significant differences were observed between the sham surgical and sham contralateral knees (**Figure 4B**).

Inflammation in chondrocytes

Immunohistochemistry staining for IL-1β and NF-κB revealed that some degree of inflammation affected chondrocytes of all groups when compared to the negative control, which showed no positive staining for IL-1β or NF-κB (**Figure 5**). However, chondrocytes of the mIAD surgical knees displayed markedly higher levels of IL-1β and NF-κB than the mIAD contralateral knees and sham surgical knees, whereas IL-1β and NF-κB levels were similar between mIAD contralateral and sham surgical knees.

Gait analysis

There was no significant difference in gait ratios between preoperative (week 0) and all postoperative (weeks 4, 8, 12, and 15) timepoints in the sham group for all six gait parameters (**Figure 6**). Similarly, for the mIAD group, there was no significant difference in gait ratios between preoperative and postoperative timepoints for maximum force, impulse, stance time, and swing time. However, gait ratios for peak pressure (P=.005) and contact area (P=.013) at 8 weeks after surgery were significantly different from preoperative values. In addition, there was no significant difference between sham and mIAD gait ratios for all indicators at corresponding timepoints.

Discussion

In this study, we developed an inflammation-driven model to induce PTOA in the Yucatan minipig by drilling non-articulating surfaces adjacent to the tibial and femoral ACL attach-

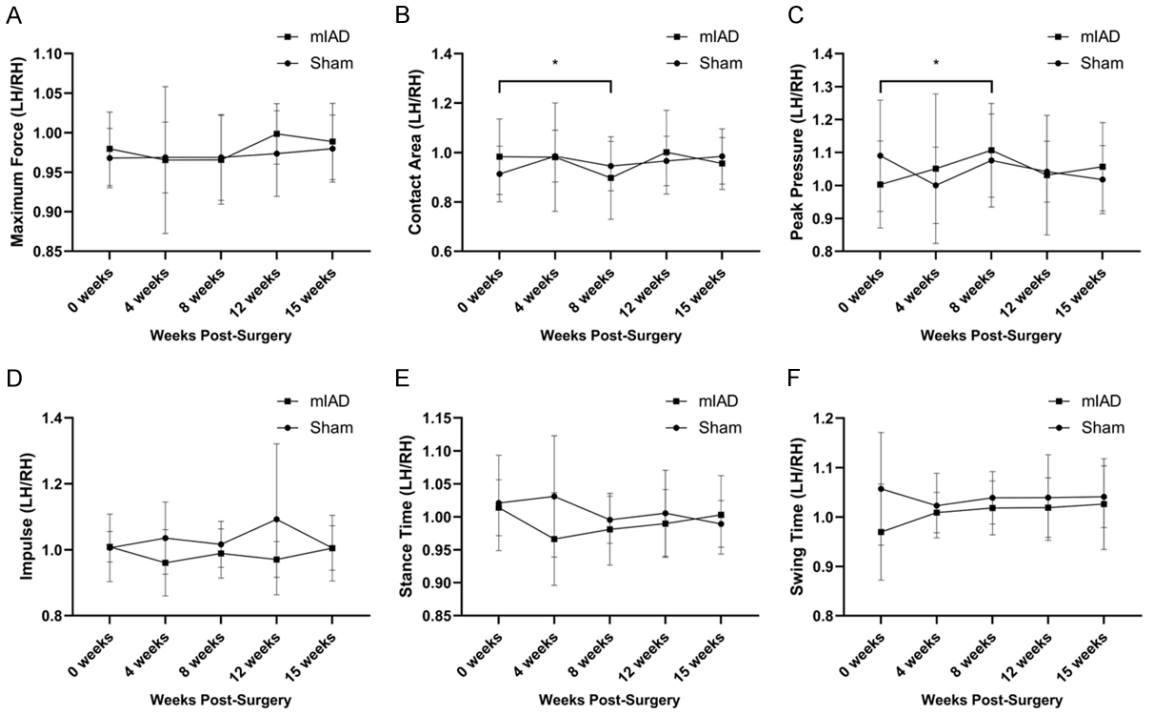

Figure 6. Line charts of the six gait indicators expressed as a ratio of left to right hind limb (A) Maximum force, (B) contact area, (C) peak pressure, (D) impulse, (E) stance time, and (F) swing time. Error bars show the mean ± SD. * indicates significant differences between gait ratios of preoperative and postoperative timepoints for the modified intra-articular drilling (mIAD) group.

ment sites. Minipigs undergoing mIAD experienced significant cartilage degeneration and demonstrated synovitis in the surgical knees. Furthermore, the synovial membrane of surgical knees demonstrated elevated IL-1β, NF-κB, and TNF-α expression, and the chondrocytes similarly expressed higher levels of IL-1β and NF-κB. Moreover, gait assessment revealed no meaningful changes in mechanical stability following mIAD. These present findings support our primary hypothesis that the mIAD procedure induces PTOA in the surgical knee through inflammatory factors but does not cause mechanical changes during gait.

Clinically, patients suffering from traumatic joint injuries are still at risk of developing PTOA despite receiving surgical treatments to repair the joint [5, 7-9]. Although the joint may be generally restabilized, many investigators speculate that catabolic inflammatory alterations remain and cause irreversible cartilage damage [5, 7, 13, 27], which may be exacerbated by residual knee motion abnormalities that persist following surgery [28-30]. Thus, studying the damaging effects of inflammation while controlling for mechanical alterations may open avenues for inflammation-targeted therapies that can reduce PTOA cartilage degeneration in a stable joint. However, there is currently no ideal animal model that can reliably separate the two factors. The present study meets the gap in current animal models and provides a model that isolates the effects of inflammation on PTOA.

The minipig provides a valuable model to study PTOA [15, 16]. Previous models induced PTOA by physically damaging soft tissues such as the ACL or meniscus through ACL transection or DMM, respectively [22, 23, 25, 31, 32]. These soft tissues are integral to maintaining joint stability and modulating the intra-articular loading environment [33, 34]. Similarly, models that induce PTOA by applying a compressive force to cause an osteochondral fracture perturb the intra-articular surfaces involved in normal joint loading [35, 36]. Thus, there is an interplay of mechanical and biological factors in these existing injury models with chronic mechanical abnormalities, likely overshadowing the effects that biological changes alone

may play [10]. Acute inflammatory response to injury through IL-1β, NF-κB, and TNF-α expression stimulates pathways that induce expression of cartilage degrading enzymes that would be heightened by the presence of altered joint contact mechanics [10]. Though Heard et al. developed the IACLR in sheep to study PTOA while controlling for altered mechanics [23], we found that their coring procedure induced additional damage to the joint when applied in minipigs. As a result, we developed the mIAD that could induce PTOA without iatrogenic injury. Similar to clinical ACL reconstruction and the coring model, our mIAD procedure involved controlled osseous drilling at the tibia and femur, albeit to an extent that is less traumatic than ACL reconstruction in order to prevent altered biomechanics [37]. Ultimately, we demonstrated that our mIAD drilling model, similar to the model described by Huebner *et al*. in rabbits, can reliably induce PTOA through inflammatory changes with limited mechanical perturbation, while also offering several advantages over the original IACLR coring model [14].

The present macroscopic and microscopic findings demonstrate that the mIAD procedure consistently induces PTOA-like joint degeneration in the cartilage and synovium. By 15 weeks, mIAD surgical joints already showed significant increases in cartilage degeneration compared to contralateral and sham groups in gold-standard measurements of cartilage damage [15]. In our PTOA model, cartilage damage was primarily located in the medial compartment of the femoral condyle and tibial plateau but was minimal in the lateral compartment. These damage patterns are similar to the results of other large-animal PTOA models [18, 22, 38-43] and, importantly, patterns described in early human PTOA [44]. In a prior PTOA minipig study using ACL transection, Karamchedu *et al.* noted significant macroscopic degeneration, namely erosion to the subchondral bone, in the medial compartment of the tibial plateau [41]. In addition, Murray and Fleming also found significant macroscopic degeneration in the medial femoral condyle of minipigs undergoing ACL transection [22]. When evaluating the medial femoral condyle microscopically, Sieker *et al.* and Costa *et al.* reported significant increases in OARSI microscopic damage scores and PTOA-like changes in chondrocytes within 4 weeks of ACL transection in the minipig [18, 43]. Our microscopic histology results align well with these prior investigations in Yucatan minipigs.

Furthermore, histological observations of synovitis present only in the mIAD surgical knee followed the abnormal features of the synovial membrane previously documented in human osteoarthritis development [12, 13]. In addition, we observed significantly higher mRNA levels of IL-1β, NF-κB, and TNF-α expression in the synovial membrane of the mIAD surgical knee compared with the contralateral. These mRNA profiles align with observations of synovitis while having known downstream catabolic effects on the cartilage extracellular matrix. Past studies have established the role of these mediators in suppressing aggrecan and collagen synthesis in chondrocytes and activating proteolytic enzymes [12, 13]. The presence of high levels of IL-1β, NF-κB, and TNF-α in the synovium in our results indicates that the cartilage is engulfed in an inflammatory environment [12]. As a result, the cartilage matrix is subject to collagenase and aggrecanase activity and subsequent degradation. In addition, IL-1β, NF-κB, and TNF-α signaling may initiate and/or perpetuate already existing chondrocyte inflammation, resulting in further biological changes that promote cartilage damage. The relative increase of IL-1β and NF-κB in chondrocytes of the mIAD knee compared to the mIAD contralateral and sham surgical knees further supports our view that inflammation is present in the cartilage. Inflammation in the cartilage is known to contribute to the activation of degenerative pathways [12, 13, 45]. However, the mechanisms of inflammation are not clear. Possible mechanisms by which intra-articular bone drilling could induce synovitis and subsequent cartilage damage include (1) residual bleeding in the joint that wound irrigation did not attenuate and (2) bone elements in the joint acting as damage-associated molecular patterns that trigger an innate immune response.

To monitor potential changes in joint loading following intra-articular drilling, load asymmetry during gait was measured. Gait analysis is a robust tool used to detect changes in joint loading and has been used extensively in both human [46] and animal [26] studies of PTOA. While others have shown prolonged hindlimb

loading asymmetry in quadrupeds immediately following procedures that destabilize the joint [26, 41], the gait indicators we evaluated were not sensitive to either mIAD or sham surgery. Although we observed transient significant differences in the contact area and peak pressure gait parameters at 8 weeks compared with 0 weeks for the mIAD group, there were no significant differences at 4, 12, or 15 weeks compared with 0 weeks. Of note, however, is that the gait ratios at 8 weeks for both contact area and peak pressure were within 10% of baseline values. The increase in the peak pressure gait ratio suggests an increase in mIAD surgical limb loading, which would contrast the direction we would expect if mechanical instability was truly present [41]. Furthermore, no significant mIAD changes were detected in the four other gait parameters. In addition, the ratios for all gait indicators were close to and centered at 1, demonstrating that hind limb loading was relatively symmetrical. When interpreted collectively, these results suggest that mIAD does not induce noticeable mechanical changes during gait and that the joint likely remains stable.

There are several advantages to the mIAD procedure as an inflammation-driven model of PTOA. Firstly, the procedure involves drilling non-articulating surfaces as opposed to transecting or injuring joint stabilizing structures, which prevents mechanical changes and allows for the isolation of cartilage damage induced by inflammation. Secondly, the procedure is easier to perform and less strenuous for the animals because it induces less mechanical damage to the joint and requires less operating time, thereby reducing recovery time from anesthesia. Thirdly, the minipig is an established pre-clinical model [16], so the present mIAD model is useful for further investigation of therapies for inflammation in PTOA. Fourthly, the drilling procedure induced PTOA in 15 weeks which allows for studying PTOA within a short timeline. In future studies, we aim to use the mIAD procedure to study the effectiveness of anti-inflammatory agents in reducing the acute post-injury inflammation and subsequent PTOA.

There are several limitations to consider. First, the PTOA degenerative changes were monitored only for 15 weeks. At this timepoint, there were minimal detectible changes in hind limb loading. However, if the cartilage damage we observed continues to worsen over time, we could expect to observe a gradual increase in limb loading asymmetry as others have noted in a similar, but more invasive model [26]. Nevertheless, any change in limb loading and presumably mechanical environment of the joint would be secondary to the inflammation-initiated damage we isolated here. Second, there was evidence of occasional damage in the mIAD contralateral and sham groups, which may represent pre-existing cartilage damage. Other minipig studies have shown similar results, with minor damage in the contralateral knee [22, 23] and sham procedures [23]. However, there was significantly more damage in the mIAD knee, which indicates that this surgical procedure successfully induced PTOA.

Conclusion

In conclusion, mIAD in a minipig model did not affect hind limb loading during gait and reliably induced PTOA at 15 weeks after surgery, primarily due to inflammatory factors. The model isolated the effects of inflammation in PTOA pathogenesis and could be used in future preclinical studies to develop inflammation-targeted PTOA therapies.

Acknowledgements

The project was funded by the Department of Defense [W81XWH1910516] and the National Institute of General Medical Sciences [P30-GM122732]. Its contents are solely the responsibility of the authors and do not necessarily represent the official views of the DoD or NIH.

Disclosure of conflict of interest

Braden C. Fleming is a founder of Miach Orthopaedics, receives royalties from Springer Publishing, and receives a stipend from the American Journal of Sports Medicine. Brett D. Owens is a paid consultant for Conmed, Miach, Vericel, and Mitek, and receives inventor royalties from Conmed and a stipend from the American Journal of Sports Medicine.

Address correspondence to: Dr. Lei Wei, Department of Orthopaedics, Warren Alpert Medical School of Brown University/Rhode Island Hospital, 1 Hoppin Street, Providence, RI 02903, USA. Tel: 401-793-8384; Fax: 401-444-6140; E-mail: Lei_Wei@brown.edu

References

[1] Narez GE, Fischenich KM and Donahue TLH. Experimental animal models of post-traumatic osteoarthritis of the knee. Orthop Rev (Pavia) 2020; 12: 8448.

[2] Brown TD, Johnston RC, Saltzman CL, Marsh JL and Buckwalter JA. Posttraumatic osteoarthritis: a first estimate of incidence, prevalence, and burden of disease. J Orthop Trauma 2006; 20: 739-744.

[3] Salonen EE, Magga T, Sillanpää PJ, Kiekara T, Mäenpää H and Mattila VM. Traumatic patellar dislocation and cartilage injury: a follow-up study of long-term cartilage deterioration. Am J Sports Med 2017; 45: 1376-1382.

[4] McKinley TO, Borrelli J Jr, D'Lima DD, Furman BD and Giannoudis PV. Basic science of intra-articular fractures and posttraumatic osteoarthritis. J Orthop Trauma 2010; 24: 567-570.

[5] Bodkin SG, Werner BC, Slater LV and Hart JM. Post-traumatic osteoarthritis diagnosed within 5 years following ACL reconstruction. Knee Surg Sports Traumatol Arthrosc 2020; 28: 790-796.

[6] Trivedi J, Betensky D, Desai S and Jayasuriya CT. Post-traumatic osteoarthritis assessment in emerging and advanced pre-clinical meniscus repair strategies: a review. Front Bioeng Biotechnol 2021; 9: 787330.

[7] Chalmers PN, Mall NA, Moric M, Sherman SL, Paletta GP, Cole BJ and Bach BR Jr. Does ACL reconstruction alter natural history?: a systematic literature review of long-term outcomes. J Bone Joint Surg Am 2014; 96: 292-300.

[8] Smith TO, Song F, Donell ST and Hing CB. Operative versus non-operative management of patellar dislocation. A meta-analysis. Knee Surg Sports Traumatol Arthrosc 2011; 19: 988-998.

[9] Schenker ML, Mauck RL, Ahn J and Mehta S. Pathogenesis and prevention of posttraumatic osteoarthritis after intra-articular fracture. J Am Acad Orthop Surg 2014; 22: 20-28.

[10] Dare D and Rodeo S. Mechanisms of post-traumatic osteoarthritis after ACL injury. Curr Rheumatol Rep 2014; 16: 448.

[11] Heard BJ, Barton KI, Abubacker S, Chung M, Martin CR, Schmidt TA, Shrive NG and Hart DA. Synovial and cartilage responsiveness to perioperative hyaluronic acid ± dexamethasone administration following a limited injury to the rabbit stifle joint. J Orthop Res 2022; 40: 838-845.

[12] Scanzello CR and Goldring SR. The role of synovitis in osteoarthritis pathogenesis. Bone 2012; 51: 249-257.

[13] Lieberthal J, Sambamurthy N and Scanzello CR. Inflammation in joint injury and post-traumatic osteoarthritis. Osteoarthritis Cartilage 2015; 23: 1825-1834.

[14] Huebner KD, Shrive NG and Frank CB. New surgical model of post-traumatic osteoarthritis: isolated intra-articular bone injury in the rabbit. J Orthop Res 2013; 31: 914-920.

[15] Little CB, Smith MM, Cake MA, Read RA, Murphy MJ and Barry FP. The OARSI histopathology initiative - recommendations for histological assessments of osteoarthritis in sheep and goats. Osteoarthritis Cartilage 2010; 18 Suppl 3: S80-92.

[16] Wang D, Cubberly M, Brown WE, Kwon H, Hu JC and Athanasiou KA. Diagnostic arthroscopy of the minipig stifle (knee) for translational large animal research. Arthrosc Tech 2021; 10: e297-e301.

[17] Xerogeanes JW, Fox RJ, Takeda Y, Kim HS, Ishibashi Y, Carlin GJ and Woo SL. A functional comparison of animal anterior cruciate ligament models to the human anterior cruciate ligament. Ann Biomed Eng 1998; 26: 345-352.

[18] Sieker JT, Proffen BL, Waller KA, Chin KE, Karamchedu NP, Akelman MR, Perrone GS, Kiapour AM, Konrad J, Murray MM and Fleming BC. Transcriptional profiling of articular cartilage in a porcine model of early post-traumatic osteoarthritis. J Orthop Res 2018; 36: 318-329.

[19] Boguszewski DV, Shearn JT, Wagner CT and Butler DL. Investigating the effects of anterior tibial translation on anterior knee force in the porcine model: is the porcine knee ACL dependent? J Orthop Res 2011; 29: 641-646.

[20] Proffen BL, McElfresh M, Fleming BC and Murray MM. A comparative anatomical study of the human knee and six animal species. Knee 2012; 19: 493-499.

[21] Kiapour AM, Shalvoy MR, Murray MM and Fleming BC. Validation of porcine knee as a sex-specific model to study human anterior cruciate ligament disorders. Clin Orthop Relat Res 2015; 473: 639-650.

[22] Murray MM and Fleming BC. Use of a bioactive scaffold to stimulate anterior cruciate ligament healing also minimizes posttraumatic osteoarthritis after surgery. Am J Sports Med 2013; 41: 1762-1770.

[23] Heard BJ, Achari Y, Chung M, Shrive NG and Frank CB. Early joint tissue changes are highly correlated with a set of inflammatory and degradative synovial biomarkers after ACL autograft and its sham surgery in an ovine model. J Orthop Res 2011; 29: 1185-1192.

[24] Percie du Sert N, Hurst V, Ahluwalia A, Alam S, Avey MT, Baker M, Browne WJ, Clark A, Cuthill IC, Dirnagl U, Emerson M, Garner P, Holgate ST, Howells DW, Karp NA, Lazic SE, Lidster K, Mac-

Callum CJ, Macleod M, Pearl EJ, Petersen OH, Rawle F, Reynolds P, Rooney K, Sena ES, Silberberg SD, Steckler T and Wurbel H. The ARRIVE guidelines 2.0: updated guidelines for reporting animal research. BMJ Open Sci 2020; 4: e100115.

[25] Kiapour AM, Fleming BC and Murray MM. Structural and anatomic restoration of the anterior cruciate ligament is associated with less cartilage damage 1 year after surgery: healing ligament properties affect cartilage damage. Orthop J Sports Med 2017; 5: 2325967117723886.

[26] Zhao R, Dong Z, Wei X, Gu X, Han P, Wu H, Yan Y, Huang L, Li H, Zhang C, Li F and Li P. Inflammatory factors are crucial for the pathogenesis of post-traumatic osteoarthritis confirmed by a novel porcine model: "Idealized" anterior cruciate ligament reconstruction" and gait analysis. Int Immunopharmacol 2021; 99: 107905.

[27] Rothrauff BB, Jorge A, de Sa D, Kay J, Fu FH and Musahl V. Anatomic ACL reconstruction reduces risk of post-traumatic osteoarthritis: a systematic review with minimum 10-year follow-up. Knee Surg Sports Traumatol Arthrosc 2020; 28: 1072-1084.

[28] Tashman S, Collon D, Anderson K, Kolowich P and Anderst W. Abnormal rotational knee motion during running after anterior cruciate ligament reconstruction. Am J Sports Med 2004; 32: 975-983.

[29] Deneweth JM, Bey MJ, McLean SG, Lock TR, Kolowich PA and Tashman S. Tibiofemoral joint kinematics of the anterior cruciate ligament-reconstructed knee during a single-legged hop landing. Am J Sports Med 2010; 38: 1820-1828.

[30] Defrate LE, Papannagari R, Gill TJ, Moses JM, Pathare NP and Li G. The 6 degrees of freedom kinematics of the knee after anterior cruciate ligament deficiency: an in vivo imaging analysis. Am J Sports Med 2006; 34: 1240-1246.

[31] Waller KA, Chin KE, Jay GD, Zhang LX, Teeple E, McAllister S, Badger GJ, Schmidt TA and Fleming BC. Intra-articular recombinant human proteoglycan 4 mitigates cartilage damage after destabilization of the medial meniscus in the Yucatan minipig. Am J Sports Med 2017; 45: 1512-1521.

[32] Huang L, Riihioja I, Tanska P, Ojanen S, Palosaari S, Kroger H, Saarakkala SJ, Herzog W, Korhonen RK and Finnila MAJ. Early changes in osteochondral tissues in a rabbit model of post-traumatic osteoarthritis. J Orthop Res 2021; 39: 2556-2567.

[33] Imhauser C, Mauro C, Choi D, Rosenberg E, Mathew S, Nguyen J, Ma Y and Wickiewicz T. Abnormal tibiofemoral contact stress and its association with altered kinematics after center-center anterior cruciate ligament reconstruction: an in vitro study. Am J Sports Med 2013; 41: 815-825.

[34] Sukopp M, Schall F, Hacker SP, Ignatius A, Durselen L and Seitz AM. Influence of menisci on tibiofemoral contact mechanics in human knees: a systematic review. Front Bioeng Biotechnol 2021; 9: 765596.

[35] Tochigi Y, Zhang P, Rudert MJ, Baer TE, Martin JA, Hillis SL and Brown TD. A novel impaction technique to create experimental articular fractures in large animal joints. Osteoarthritis Cartilage 2013; 21: 200-208.

[36] Goetz JE, Fredericks D, Petersen E, Rudert MJ, Baer T, Swanson E, Roberts N, Martin J and Tochigi Y. A clinically realistic large animal model of intra-articular fracture that progresses to post-traumatic osteoarthritis. Osteoarthritis Cartilage 2015; 23: 1797-1805.

[37] Noronha JC and Oliveira JP. Inside-out tibial tunnel drilling technique for all-inside anterior cruciate ligament reconstruction. Arthrosc Tech 2018; 7: e373-e377.

[38] Zhang L, Peng H, Feng M, Zhang W and Li Y. Yeast microcapsule-mediated oral delivery of IL-1beta shRNA for post-traumatic osteoarthritis therapy. Mol Ther Nucleic Acids 2021; 23: 336-346.

[39] Smith GN, Mickler EA, Albrecht ME, Myers SL and Brandt KD. Severity of medial meniscus damage in the canine knee after anterior cruciate ligament transection. Osteoarthritis Cartilage 2002; 10: 321-326.

[40] Wei B, Zong M, Yan C, Mao F, Guo Y, Yao Q, Xu Y and Wang L. Use of quantitative MRI for the detection of progressive cartilage degeneration in a mini-pig model of osteoarthritis caused by anterior cruciate ligament transection. J Magn Reson Imaging 2015; 42: 1032-1038.

[41] Karamchedu NP, Murray MM, Sieker JT, Proffen BL, Portilla G, Costa MQ, Molino J and Fleming BC. Bridge-enhanced anterior cruciate ligament repair leads to greater limb asymmetry and less cartilage damage than untreated ACL transection or ACL reconstruction in the porcine model. Am J Sports Med 2021; 49: 667-674.

[42] Karamchedu NP, Fleming BC, Donnenfield JI, Proffen BL, Costa MQ, Molino J and Murray MM. Enrichment of inflammatory mediators in the synovial fluid is associated with slower progression of mild to moderate osteoarthritis in the porcine knee. Am J Transl Res 2021; 13: 7667-7676.

[43] Costa MQ, Murray MM, Sieker JT, Karamchedu NP, Proffen BL and Fleming BC. Peripheral shift in the viable chondrocyte population of the medial femoral condyle after anterior cru-

ciate ligament injury in the porcine knee. PLoS One 2021; 16: e0256765.
[44] Zhong Q, Pedoia V, Tanaka M, Neumann J, Link TM, Ma B, Lin J and Li X. 3D bone-shape changes and their correlations with cartilage T1rho and T2 relaxation times and patient-reported outcomes over 3-years after ACL reconstruction. Osteoarthritis Cartilage 2019; 27: 915-921.
[45] Mehana EE, Khafaga AF and El-Blehi SS. The role of matrix metalloproteinases in osteoarthritis pathogenesis: an updated review. Life Sci 2019; 234: 116786.
[46] Wellsandt E, Zeni JA, Axe MJ and Snyder-Mackler L. Hip joint biomechanics in those with and without post-traumatic knee osteoarthritis after anterior cruciate ligament injury. Clin Biomech (Bristol, Avon) 2017; 50: 63-69.